Acta of Bioengineering and Biomechanics
Vol. 20, No. 2, 2018

Original paper
DOI: 10.5277/ABB-01107-2018-02

Effect of porosity on the structure, mechanical properties and cell viability of new bioceramics as potential bone graft substitutes

MEHTAP DEMIREL[1], BUNYAMIN AKSAKAL[2]*

[1] Adiyaman University, Vocational School of Technical Sci, Adiyaman, Turkey.
[2] Yildiz Technical University, Faculty of Chemical and Metallurgy,
Department of Metallurgy and Mater Engineering, Istanbul, Turkey.

Porous and alternative biografts for possible usages in orthopaedic applications were synthesized by the substitution of gelatin (G), cuttlefish backbone (C), meerschaum sepiolite (S) and hydroxyapatite (H). The effects of different proportions of the Gelatin substitutions on the mechanical properties and structure and cell viability properties of the fabricated biografts were investigated. Throughout the structure and mechanical evaluations, it was found that Gelatin substitution in the fabricated biografts increased the total porosity fraction, particularly for C13G75 and S13G75 biografts. Scanning Electron Microscope (SEM), X-ray diffraction (XRD) and Fourier Transform Infrared Spectroscopy (FTIR) were used for characterization of the synthesized biografts. Furthermore, the cell viability tests for the synthesized biografts were carried out by using the osteoblast cell culture. Throughout the analysis, the synthesized C13G75 and S13G75 biografts generated the highest porosity and better correlation between mechanical properties and structural results contributing with highest cell viability rates.

Key words: *bone graft; hydroxyapatite; sol-gel; porosity; mechanical properties*

1. Introduction

Bone is divided into two parts (compact cortical, cancellous (trabecular)) that differ in their density and porosity [1]. One of the morphological components of bone and trabecular bone has 1 mm radius, on average, and 50–90% porosity, and envelopes cortical bone. The average density, hardness and structural Elasticity modulus of trabecular bone are 0.30–1.85 gr/cm^3, 0.234–0.760 GPa, 6.9–25 GPa, respectively [2], [3]. In addition, cortical bone is a tightly packed, nonporous structure having a maximum density of 1.8 g/cm^3, 3–12% porosity, surrounded by haversian channels. In several recent studies, sea-derived products were used to strengthen the inorganic skeletal structure [4]–[11]. Sea-derived products are preferred due to their structural resemblance to human bone and highly macroporous frame that enables the angiogenesis formation of capillary vessels [4]. The biomineralization structure of human bone is similar to that of some sea-derived products like cuttlefish and mother of pearl [5]. The inorganic parts of the cuttlefish back bone is anisotropic (like lamella) and consists of mineralized porous calcium carbonate ($CaCO_3$). Its structure corresponds to human bone [12] and shows several biocompatibility properties.

Previous studies reported the effects of pore structure on the mechanical properties and usefulness in biomaterials. It was reported that the pore size and porosity rate increases the cell generation that leads to easier bone generation and resulting in poorer mechanical properties [13], [14]. To obtain an optimum porous structure in biografts, besides the main compounds, polymers that help to form the pores were used. It was reported that if the polymers are used in

* Corresponding author: Bunyamin Aksakal, Yildiz Technical University, Faculty of Chemical and Metallurgy, Department of Metallurgy and Mater Engineering, 2334 Istanbul, Turkey. Phone: +90 0212 3834662, e-mail: baksakal@yildiz.edu.tr

Received: February 2nd, 2018
Accepted for publication: May 15th, 2018

Table 1. Chemical compositions of the produced biograft and groups (H, S and C)

Biografts	H [wt%]	S [wt%]	C [wt%]	G [wt%]	KH_2PO_4 [wt%]	Na_2CO_3 [wt%]	P_2O_5 [wt%]
H30G20	30	–	–	20	10	20	20
H30G30	30	–	–	30	10	15	15
H30G40	30	–	–	40	10	10	10
H13G75	13	–	–	75	2	5	5
M30G20	–	30	–	20	5	5	10
M30G30	–	30	–	30	5	10	5
M30G40	–	30	–	40	5	5	5
M13G75	–	13	–	75	2	5	5
C30G20	–	–	30	20	15	20	15
C30G30	–	–	30	30	10	15	15
C30G40	–	–	30	40	5	15	10
C13G75	–	–	13	75	2	5	5

the nanofibrous structure, a good connection between macropores is provided [15], [16]. Polymer compounds such as gelatin, alginate, montmorillonite, when added to bioceramics like HA, β-TCP, were proven to improve the mechanical and biological properties of the scaffold structure [17]–[24]. Also, by using sol-gel method, various ceramic powders such as ZrO_2-CeO_2 and ceria-stabilized zirconia at various pH conditions were obtained for potential applications in prosthetic dentistry [25], [26].

There are some other methods that enable obtaining thin layers and coatings with adequate adhesion to metallic or ceramic implants with useful surface properties that enhance osteointegration and biocompatibility [27]–[31].

Hard tissue applications particularly need better properties, structure and tissue response combinations. Although previous studies reported alternative bone grafts, some deficiencies seem to affect the correlation between the porosity, mechanical properties, structure and cell viability of the syntesized artificial bone grafts that to be replaced with defected bone. In this study, alternative biografts with different substitutions, e.g., hydroxyapatite (H), cuttlefish backbone (C) and sepiolite (S) were synthesized using sol-gel method and effects of porosity on their mechanical properties-structure and cell viability were determined.

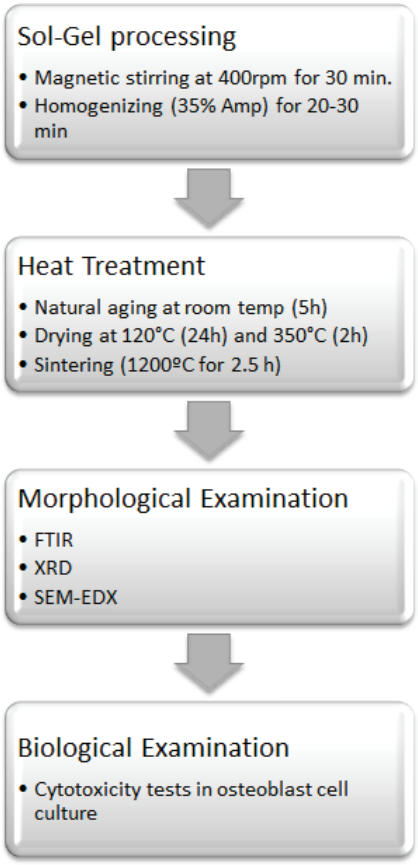

Fig. 1. Experimental flow chart

2. Materials and methods

Sol-gel method was used to synthesize new biografts. They were fabricated by the substitution of hydroxyapatite (13–30 wt. %), cuttlefish bone (13–30 wt. %), sepiolite (13–30 wt. %) and the gelatin (20–75 wt. %) in order to provide the porosity. Na_2CO_3 and P_20_5 were added into all biografts to increase the gelation during the sol-gel process and KH_2PO_4 – to ease the sinterability. Figure 1 shows a flow chart of experimental processes and Fig. 2 illustrates the initial sol-gel compositions of the all biografts produced. Following the synthesis via sol-gel method, all biografts were dried in a furnace at 120 °C for 24 hours. All compounds were mixed with ethanol and distilled water at room temperature and at

an ambient atmosphere for 30 minutes with a magnetic stirrer until a gel was obtained. Afterwards, a homogenous gel structure was acquired by mixing in a homogenizer (Cole Parmer, 750W) at 37 °C and 35% Amp intensity for 30 minutes. The gel was then aged at room temperature for five hours. For the pore structures or porous biografts the to be completed, gelatin was removed from the environment and the samples were aged at room temperature and then dried in an oven at 120 °C. Then, all samples were aged at 350 °C in vacuum atmosphere for two hours prior to sintering to eliminate any residual humidity and evaporate the gelatin to obtain pore structure. After drying, as a final stage, the sintering was performed at 1200 °C for 2.5 hours under a vacuum atmosphere.

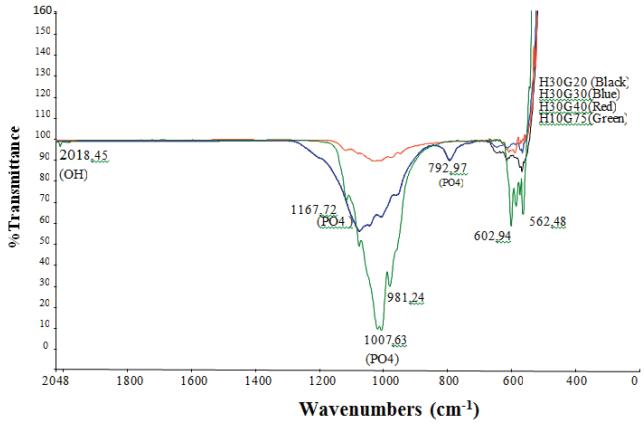

(a)

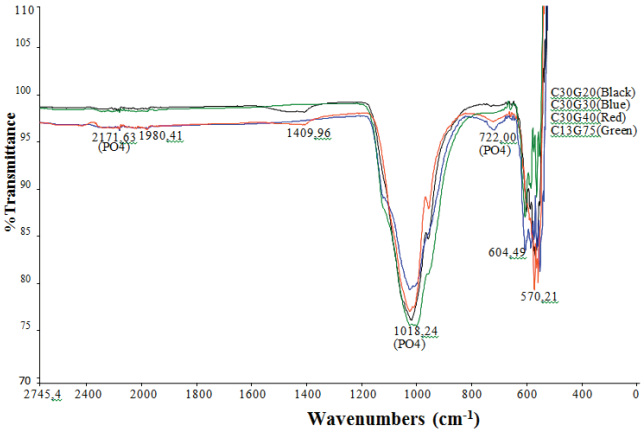

(b)

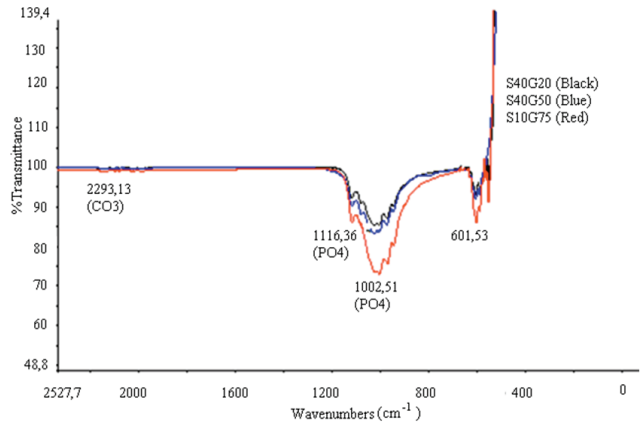

(c)

Fig. 2. FTIR spectographs of (a) H30G20, H30G30, H30G40 and H13G75, (b) C30G20, C30G30, C30G40 and C13G75 and (c) S30G20, S30G40 and S13G75 biografts

To determine the properties of the fabricated biografts, after sintering the compression (Shimadzu – 50 kN) and Vickers microhardness (Leica) tests were conducted. The surface morphology and fractograph of the hydroxyapatite, cuttlefish backbone and sepiolite-based biograft structures with various porosity rates were performed by SEM (JOEL, JSM-7001F). The synthesized biografts were characterized by XRD (BRUKER D8 ADVANCE (λ = 1.5406 Å) and FTIR (ALTI Unicam WATTSON 1000). X-Ray spectrums were recorded at 2q = 3–70° range, 2 °/min scanning rate and 1 second fixed time interval. FTIR analysis was performed at 4000–400 cm^{-1} wave ranges with 2 cm^{-1} resolution. Three samples were used to characterize and determine the mechanical and structural properties of the fabricated biografts.

To investigate the toxic effects, five fabricated biograft samples in each group were subjected to cell viability tests in different culture environments (osteoblasts). Osteoblast is an immature cell where turns into immature bone cells during the process. In the cell viability tests, the biografts were dissolved in a solvent and to decrease concentrations of the mixture to 1mg/ml, DMEM was added to dilute. The viability evaluations of the cells were executed with a MTS (cell proliferation assay) (3-(4,5-dimetiltiazol--2-yl)-5-(3-carboxymetoxyfenil)-2-(4-sulfofenil) tetrazolium, (Cell Titer 96 Aqueous One Solution Assay) test in 96 well culture plates. Cells were then planted onto 96 blank plates with a 100 µl culture environment. Each plate contained 5000 cells and was left to grow for 24 hours. The following day, the culture environments were withdrawn and the desired concentrations were applied to the cells in the culture environments (DMEM). Culture environment (DMEM) was used as a negative control and DMSO (20%) was used as a positive control. When the incubation time was completed, the culture environments in the wells were withdrawn and added to the blanks to obtain the 10 µl MTS + 100 µl culture environments. Cells that were subjected to MTS were left to incubate at 37 °C in 5% CO_2 for 2 to 3 hours. After incubation, the cell vitality was verified by a petri dish reader (Elisa plate reader). The toxicity of the grafts was investigated by

counting the cells in bakers at different concentrations (0.1–0.5 µm/ml) and at 24 to 72 hours time intervals. Porosity measurements [%] of the biografts (H, C and *S*-based) were carried out by using the Archimedes' principle.

3. Results

Some surface modifications and tissue scaffolds were previously produced that are easily removed and do not disturb the structure in obtaining a porous structure [22]–[24]. In this study, new synthesized biograft alternatives are presented; hydroxyapatite, sepiolite and cuttlefish derived compounds were mixed with sintering materials (CaO, Na_2CO_3 and KH_2PO_4) and a polymer (gelatin) to acquire a porous structure. Microscopic images of these structures were investigated. Characterization analysis and *in vitro* experiments were carried out to validate and compare their morphological and cell viability properties.

The results suggest that porosity and diameters increase along with an increase of the amount of gelatin. The lowest pore amount was obtained with a 10 wt. % G substituted biografts and the highest pore amount was obtained with 75 wt. % G substituted biografts. The highest porosity (50.5%) was reached in the S13G75 biograft as the lowest porosity (15.3%) was

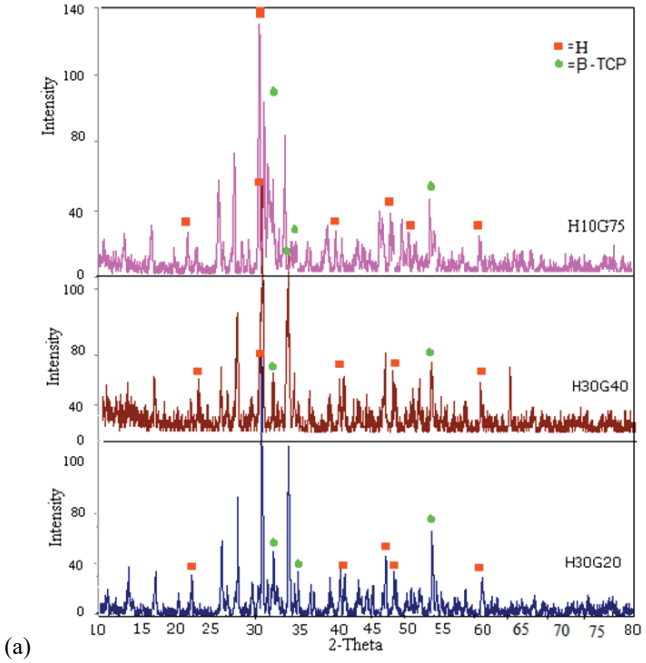

(a)

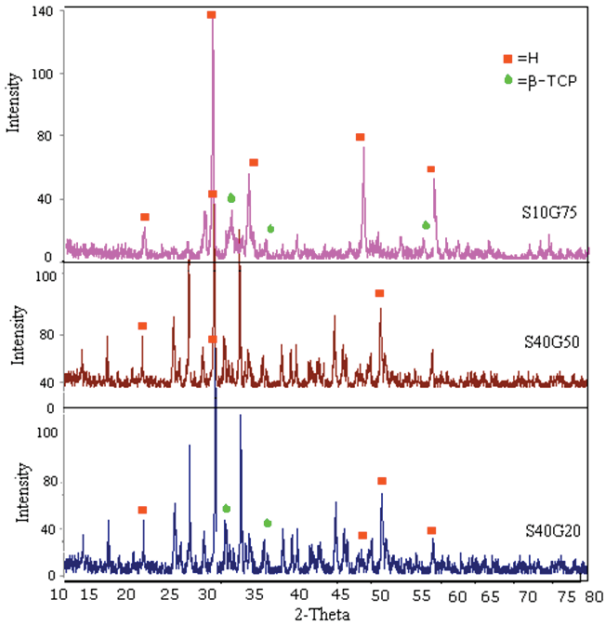

(b)

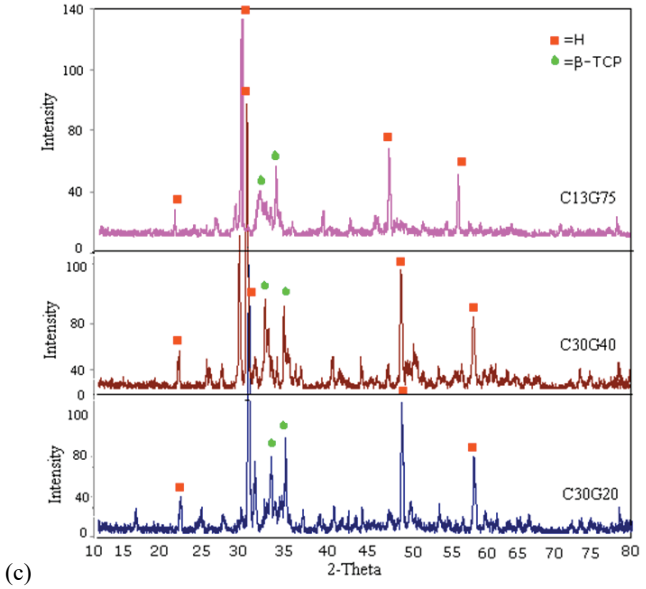

(c)

Fig. 3. XRD spectrums of (a) H30G20, H30G40 and H13G75, (b) C40G20, C40G40 and C10G75 and (c) S30G20, S30G40 and S13G75 biografts

obtained in the H30G20 biograft. Combined FTIR spectrographs of various biografts were plotted and presented in Figs. 2a–c. FTIR analysis of the biografts (10–30 wt. % H-based and 20, 30, 40, 75 wt. % G) show characteristic bands for CaOH and also M-O regarding their metal compounds. Figures 3a–c show the combined XRD spectrums of H-based (a), cuttlefish backbone (b) and sepiolite based (c) porous biografts with gelatin substitution from 13 to 75 wt. %.

Figures 4a–c show the SEM images of H-based and 13–75 wt. % G substituted biografts. Figure 4a and b show irregular morphology with hill flakes on the surface as well as little porous structure structures in H30G20 and H30G40 H-derived and 20 and 40 wt. % gelatin-substituted biografts. These biografts show the formation of the nonhomogeneous structure with low porous structures. Figure 4c shows SEM images of sample H13G75 (13 wt. % H based and 75 wt. % gelatin) biograft. Figures 5a–c show SEM images of the synthesized biograft with cuttlefish backbone (C-derived) biografts. The biograft C30G20 (C-derived) and 20 wt. % G-substituted biografts are shown in Fig. 5a. SEM image of the C30G20 biograft shows cracky but regular low porous structure with connected network between the powders. Figure 5b shows the SEM image of C30G30 (30 wt. % cuttlefish backbone-based and 30 wt% gelatin-substituted biograft), having high porous structure. Figures 6a–c shows the SEM images of the S-based (13 to 75 wt. % gelatin substituted porous biografts. Figure 7 show the per cent porosity (%) distributions of the fabricated biografts. From the overall results, H-substituted biografts showed the lowest porosity (15.3%), and the C- and S-substituted biografts provided the highest porosities (45 and 50.5%), especially at 75 wt. % G substitutions.

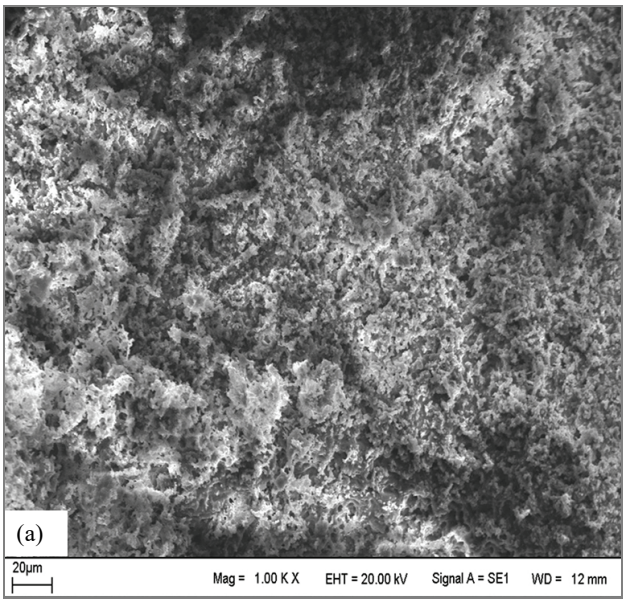

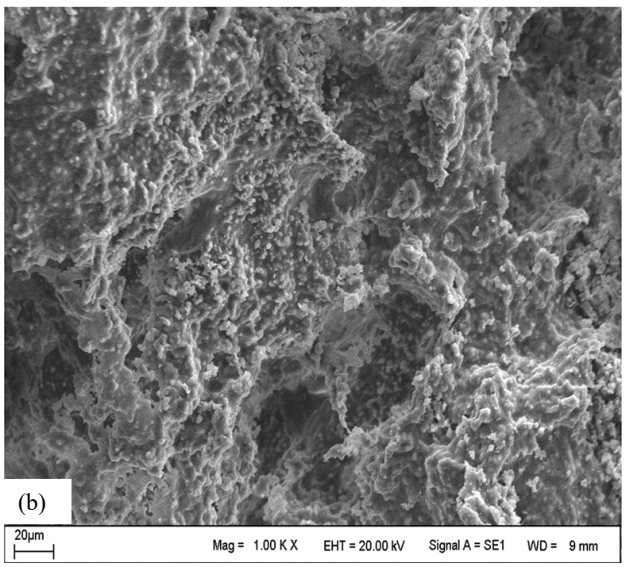

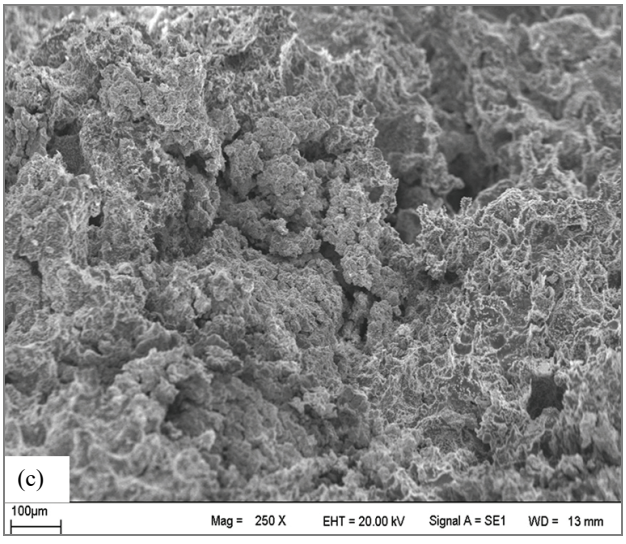

Fig. 4. SEM images of (a) H30G20, (b) H30G30, (c) H13G75 biografts

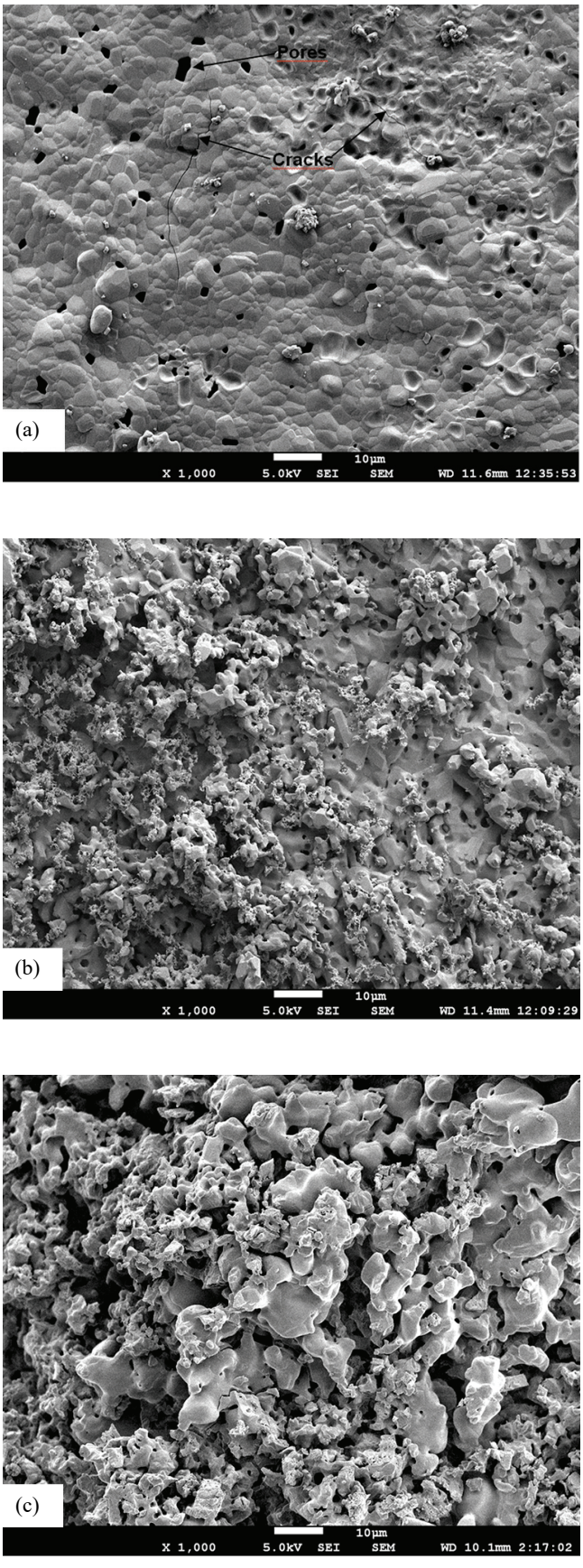

Fig. 5. SEM images of (a) C30G20, (b) C30G30 and (c) C13G75 biografts

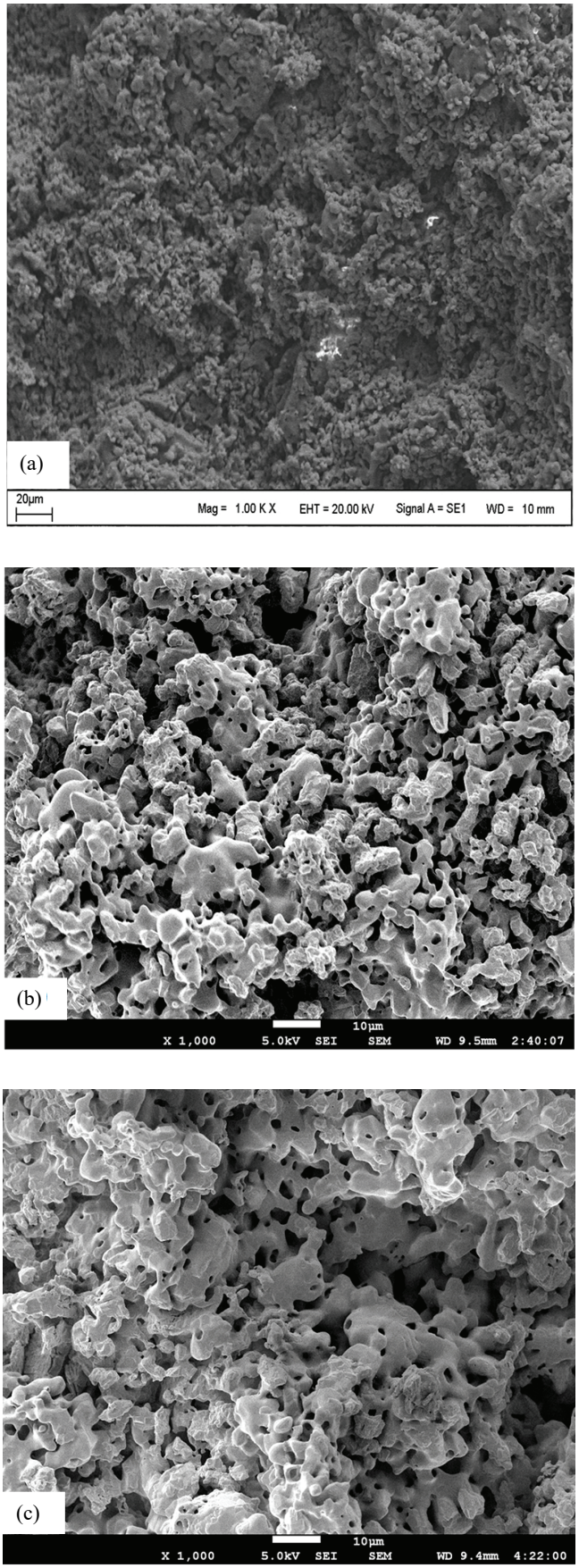

Fig. 6. SEM images of (a) S30G20, (b) S30G30, (c) S13G75 biografts

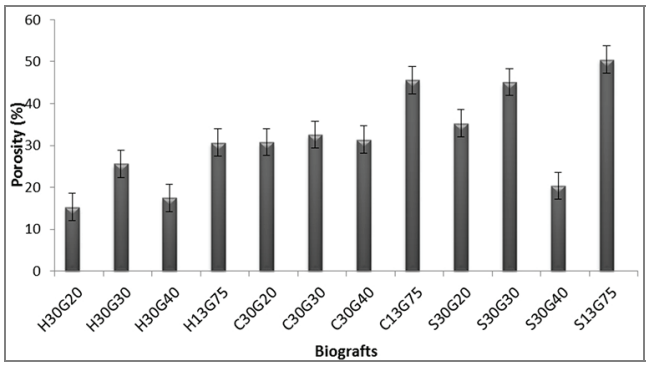

Fig. 7. Porosities [%] of H, C and S-based biografts

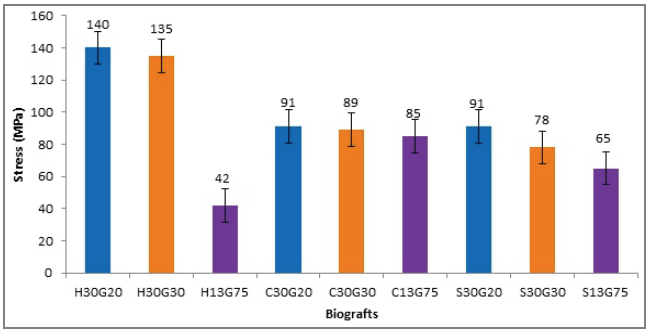

(a)

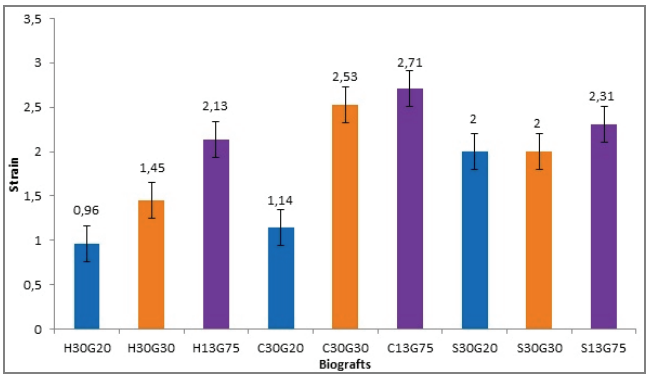

(b)

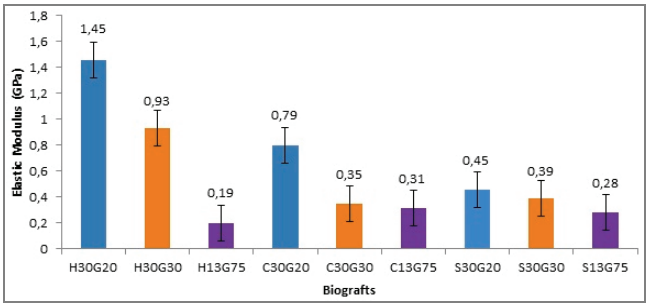

(c)

Fig. 8. Variation of ultimate stress (a), strain (b) and elasticity modulus (c) of the synthesized biografts with different substitutions

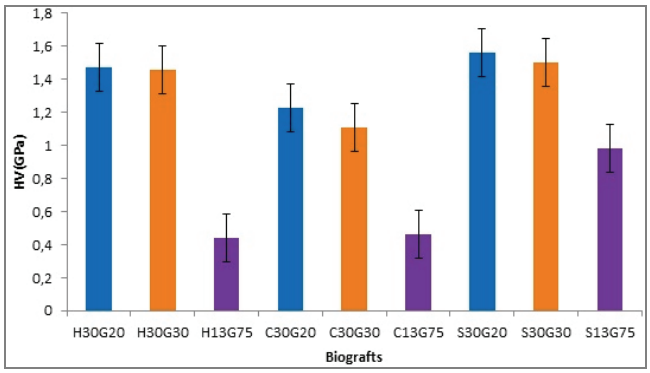

Fig. 9. Variation of hardness of the synthesized biografts with different substitutions

Mechanical tests including compression and hardness results were given in Figs. 8a–c and Fig. 9, respectively. Compression test results shown in Figs. 8a–c revealed that the ultimate stress and elasticity modulus values were decreased and displacement [%] increased with increasing gelatin ratio and porosity (Figs. 8a–c). In all synthesized H-, C- and S-based-biografts, hardness values also diminished along with an increased gelatin substitution ratio and porosity (Fig. 9). Comparing the structural results of all biograft to SEM views given in Figs. 4–6, the ultimate stress and hardness results are in good agreement. For example, as can be seen in Figs. 8a–c and Fig. 9, the stress, elastic modulus and hardness values decrease particularly in H-based grafts with increased gelatin substitution (wt. %) and decreased porosity (%) due to worse interconnections and cracks between the powders obtained after sintering. Because of better sintering between the used powders for the C- and S-based biografts, mechanical properties did not decrease as much as decreased in H-based biografts. In Figures 10a–c, the fractographic SEM views of some synthesized biografts (H30G20, S13G75 and C13G75) are shown. Based on those views, it was determined that H30G20 shows the lowest and S13G75 – the highest porous structure. As shown in Figs. 11a and b, for the biografts of both compositions H30G20 (Fig. 11a) and H13G75 (Fig. 11b), the cell vitality ratios are high.

Figures 12a and 12b show the results of cell viability test for C30G20 and C13G75, cuttlefish and G-substituted biografts. The osteoblast cells were measured at 0.1–0.3 µg/ml concentrations. No toxic effects were observed at 0.1–0.3 µm/ml according to the increase in live cell density at the end of the third day. The C13G75 biograft also exhibited an increase in the density of cells at 0.1 µm/ml at the end of the third day. Figure 13b shows the cell viability ratio of the S10G75 biograft measured above 100 at the end of the third day. In addition, the S30G20 and S13G75

(13 wt. % sepiolite and 20–75 wt. % gelatin) biografts show that the cell viability ratio was decreased with incubation times and concentrations (Fig. 13a).

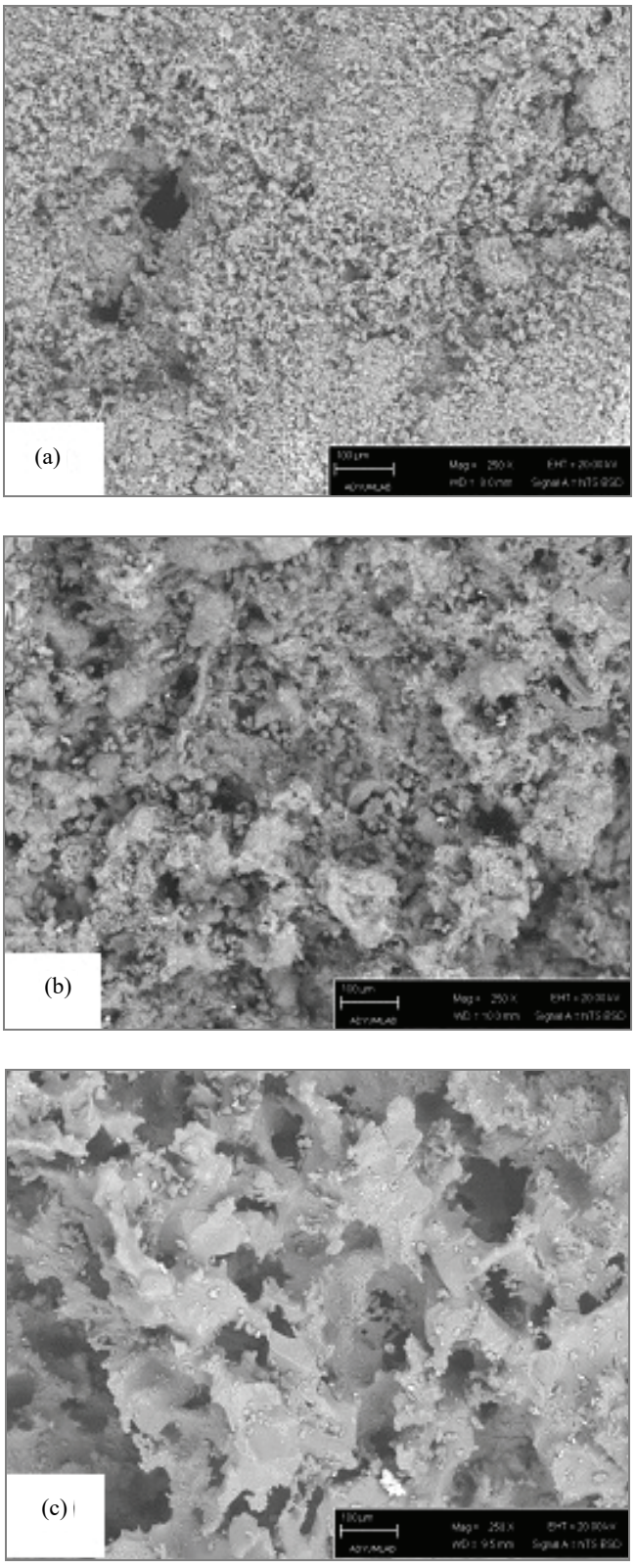

Fig. 10. SEM views of fracture surfaces for:
(a) H30G20, (b) C13G75 and (c) S13G75 biografts

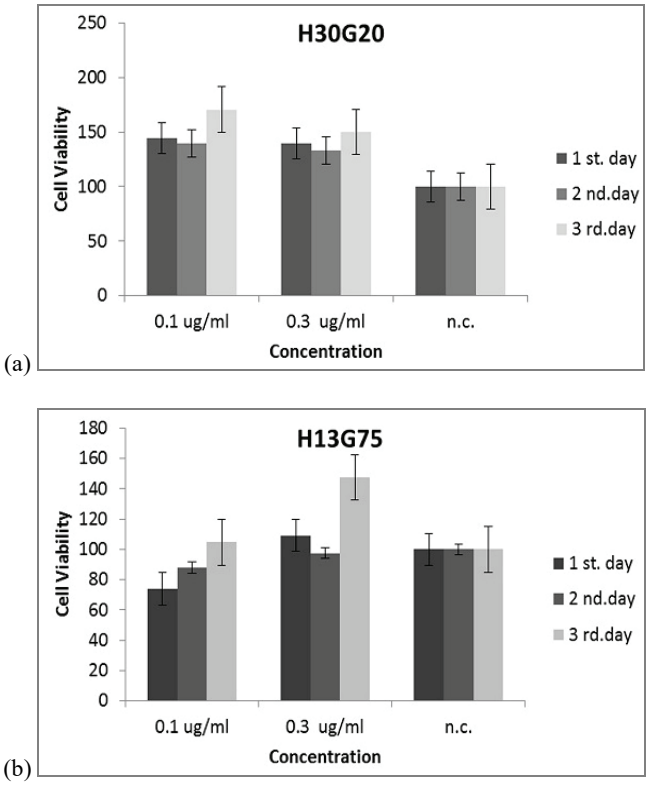

Fig. 11. Comparisons of cell viability changes in time and with different concentrations for:
(a) H30G20, (b) H13G75 biografts

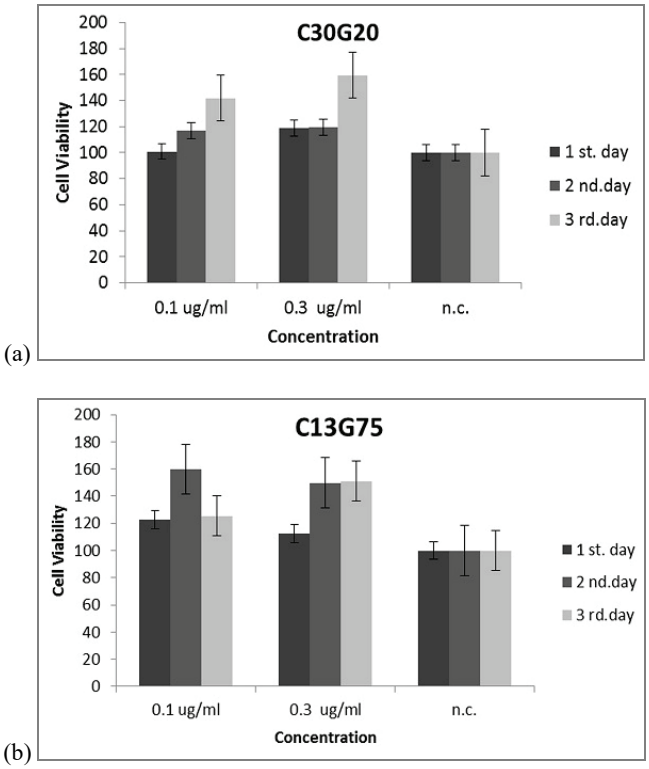

Fig. 12. Comparisons of cell viability changes in time and with different concentrations for:
(a) C30G20, (b) C13G75 biografts

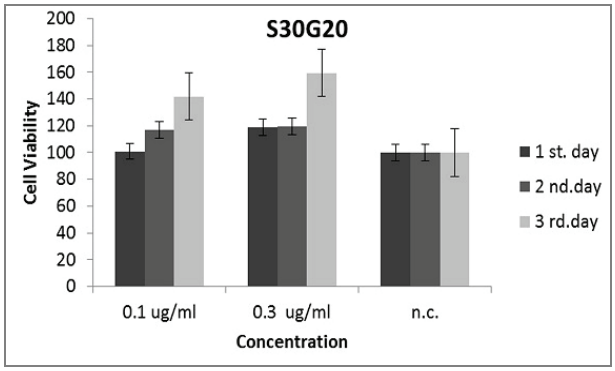

(a)

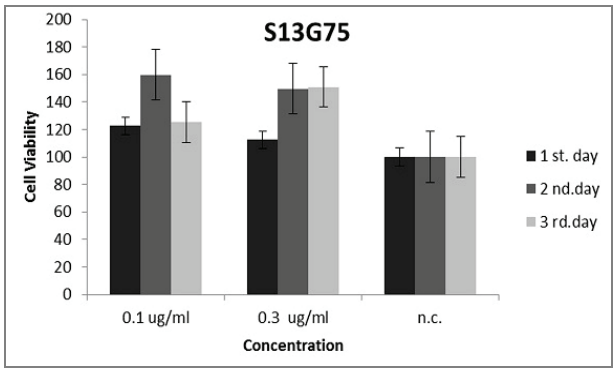

(b)

Fig. 13. Comparisons of cell viability changes in time and with different concentrations for: (a) S40G20, (b) S13G75 biografts

4. Discussion

The peaks shown in Figs. 2a–c, between 1167 and 792 cm^{-1} represent PO_4^{-3} while the peak at 2018.85 cm^{-1} represents characteristic hydrogen originated OH^- and peaks between 602 and 560 cm^{-1} represent M-O bands (Fig. 2a). Figure 2b shows the FTIR spectrums of C30G20, C30G30, C30G40 and C13G75 biografts, including 13 wt. % cuttlefish backbone C-substituted with 75 wt. % gelatin (G). Because of the presence of cuttlefish backbone and gelatin, all biografts show similar peaks while in the range of 2171.63–1409.96 cm^{-1} due to $(CO_3)^{-2}$ compound's broad and intense tension peaks. Also, the peaks observed in between 1018.24–722 cm^{-1}, $(PO_4)^{-3}$ and 1018.24 cm^{-1} appeared to be the sharpest peaks. The effects of both sepiolite and gelatin substitutions into the sol, physical and mechanical properties of the biografts were investigated. Figure 2c shows the FTIR results of the sepiolite and gelatin-substituted biografts. As can be seen from the Figure, a broad and low intensity peak at 2293.13 cm^{-1} is present due to the $(CO_3)^{-2}$ compound and in between 1116.36–601.53 cm^{-1} a $(PO_4)^-$ peak (the sharpest peak is obtained at 1116.36 cm^{-1}). Similar morphologies and crystallinities were also reported in [32].

According to the XRD analysis of the synthesized porous biografts, H and β-TCP phases are present. PO_4^{-3} and CO_3^{-2} peaks obtained in FTIR spectra are consistent with the XRD results. Since atoms which constitute molecules are always in motion, vibrations causing molecular shifting, rotation around an axis and the periodical bending-stretching of bonds or periodical changes of angles in molecules. Peaks of FTIR analysis are obtained regarding such vibrational movements. FTIR results of all biografts show PO_4^{-3} and CO_3^{-2} peaks between 600 and 2018 cm^{-1} with regards to H, KH_2PO_4 and Na_2CO_3 compounds. It was found that the width and length of the peaks decrease along with an increase pore amounts by increasing the G amount. In addition, it is confirmed that as peak width and length decreases, the grain size and crystallinity of the biografts also decreases (Figs. 2 and 3). While all H-based compounds show similar peaks in the same range, Fig. 2a shows that as the percentage of G amounts increases, peak intensity also increases. Also, due to an increase in the peak intensity caused by G amounts, OH^- peaks that are not visible for H30G20, H30G30 and H30G40 biografts become visible for the H13G75 biograft. When C- and S-based grafts are considered, as G substitution rate increases, the peaks get sharper with the sharpest peak obtained for the 75 wt. % G added C- or S-based biografts.

From XRD spectras shown in Fig. 3a, it is seen that H and β-TCP structures are formed, H-based and 20, 30, 40 and 75 wt. % gelatin-substituted biografts. In Fig. 3b, XRD spectra of 30 wt. % cuttlefish-based and 20 to 75 wt. % gelatin added C30G20, C30G40 and C13G75 biografts are given. From the obtained results, it was determined that C30G20 and C30G40 biografts give H ve β-TCP phases at the same angle and narrow-sharp peaks are observed. XRD results of S30G20, S30G40 and S13G75 sepiolite-based (20 to 75 wt. % G containment) biografts are given in Fig. 3c. All the peaks seen in the spectrums for the cuttlefish bone-based biografts correspond mainly to hydroxyapatite (H) and β-TCP.

When the XRD results of H30G20, H30G40 and H10G75 biografts are compared to the SEM images, the results may be interpreted with G substitution ratio, crystallinity and grain size decrease due to the increase in porosity. XRD results of sepiolite-based grafts with narrow and sharp peaks show that S40G20 and S40G40 biografts produced highly crystalline structure and large grains. On the other hand, XRD

analysis of the S13G75 biograft gives the peaks of H and β-TCP of similar angles with S40G20 and S40G40. However, the peaks are broader and shorter for the high porous structures. In the C backbone-substituted biografts, as the G amount increases, the intensity of the peaks decreases and the width and irregularities increase.

Figure 4c shows SEM images of the C13G75 (13 wt. % cuttlefish backbone based with 75 wt. % G) biograft. From the images, well homogenous, well connected porous as well as an intense structure is observed in the macroporous structure of C13G75 biograft. SEM images of the H30G20 and H30G30 biografts shown in Figs. 4a–c (H-derived and 20 and 30 wt. % G) reveal the process of sintering does not-proceed well the surface layer is of low porosity (Figs. 4a–b). However, although some cracks are observed, better structure is seen in the H13G75 (Fig. 4c) with smaller and spherical pores with different sizes and porosities. The structure exhibits a hill-like surface and thus micro sized pores due to the amount of G evaporated from the structure. Also, as can be seen from the morphology, there are exist no clear pore boundaries nor homogeneous porous structure at around the smooth areas. When compared to H-based biograft with 75 wt% gelatin addition is it can be commented that as the G amount increases up to 75 wt. %, pore size and porosity also increase but the bonds between pores seem weaker. As can be seen based the other synthesized biograft C30G20 (Fig. 5a), pore size is variable and small pores are present in addition to the larger pores. Small pores are also observed to be aggregating around intermediate zones during the liquid phase transformation as shown in Fig. 5a. In addition, the powders seem to disperse relatively homogeneously and produce good porous structure. However, compared to C30G20, the C30G30 biograft has a similar porous structure with wider and spherical pores having a good network bonding between the powders (Fig. 5b). As for cuttlefish backbone-based and 13–75 wt% G added biografts, while the G amount increases, the pore sizes also increase but the powder bonding weakens. Such porosity would be helpful in body environment, because when there is a fracture in a bone, cytokine and growing agents produce osteoprogenetor cells to migrate to the damaged area and transform into osteoblasts where controlling cell and ECM production [34].

Figure 6a shows the SEM image of the S30G20 biograft (30% S and 20% G). SEM image of the S40G20 biograft reveals that a macroporous structure exhibits good interconnections between the pores. Better network and interconnections between the powders, porosity and homogeneity are observed in S30G20, S30G30 and S30G75 biografts than in H-based ones. From the SEM image of (S30G30, 30 wt. % S and 30 wt. % G) biograft shown in Fig. 6b, the hill-like porous structure appears. Figure 6c shows the SEM image of the S13G75 (13 wt. % S and 75 wt. % G) biograft indicating the macropores obtained due to a good liquid phase sintering. The SEM image of S13G75 (13 wt. % S and 75 wt. % G) biograft is given in Fig. 6c. The S13G75 biograft exhibits a very good porous structure with the pores being interconnected with bonding between the powders. As also shown in SEM views (Fig. 7), it can be seen that the highest porosities were found in the syntesized biografts C13G75, S30G30 and S13G75 and the lowest ones – in the biografts H30G20, H30G40, S30G40, respectively. Increasing the G substitution up to 30 wt. % did not always increase the porosity, however, decreasing the S amount down to 13% and increasing the G up to 75 wt. %, caused the porosity to increase up to 50.5%. The network between the pores also seems to be good indicating that there was a liquid phase sintering. Ultimate stress and strain (%) and elasticity modulus results given in Figs. 8a–c were plotted throughout compression tests. From the plotted results, it was shown that the ultimate stress and elasticity modulus values were decreased along with increasing gelatin ratio and porosity (Figs. 8c and 7). Hardness values were also diminished along with in increased gelatin ratio and porosity (Fig. 9).

Comparing fractographic SEM views to the compression test results, good correlation were observed between the fracture surfaces and strengths, e.g., H30G20 exhibits the highest and C13G75 – the lowest stress. It is also interesting that S13G75 and C13G75 (Figs. 10b and 10c) exhibit more porous and ductile structure than H30G20 (Fig. 10a). It is also proven by comparison of the strain values given in Fig. 9, where C13G75 gave the highest strain (2.71) and H30G20 produced the lowest strain (0.96). It is also worth presenting the biografts exhibiting the lowest (S13G75) and highest (C13G75) elastic modulus, as given in Fig. 8c.

Cuttlefish backbone is comprised of $CaCO_3$ and $CaPO_4$ and contains natural materials which are easily provided worldwide. Such materials are cheap and easy to transform into the H even at low temperatures. The cuttlefish bone maintains the thermal stability of H even up to temperatures above 1350 °C and it does not lose its porous structure. Furthermore, it is suitable for physiological activities, such as tissue regeneration, since it has an optimal pore size and strong bonds between those pores [6]. It also shows high bioactivity

in vitro tests and shows good biocompatibility with osteoblast cells. Due to such properties, the porous structure was easily obtained by substituting various ratios of gelatin to Cuttlefish backbone. Obtained porous biografts were subjected to cell viability tests at 0.1 and 0.3 μm/ml concentrations for 72 hours.

Results of the cell measurements taken from the H30G20 biograft at different concentrations and times showed an increase in the number of live cells at the end of the third day for 0.1 μm/ml but the live cell ratio decreased on the third day for 0.3 μm/ml. In the case of the H13G75 biograft (Fig. 11b), the cell viability rate increased linearly at 0.1 μm/ml and such increment was continued at a 0.3 μm/ml concentration with the cell viability rate even at the end of the third day (measured to be over the 100 unit). Such increases are more obvious at the end of third day for the H13G75 biograft, as shown in Fig. 11b which indicates a lower cell viability rate.

Cell viability tests of synthesized H30G20, H13G75, C30G20, C13G75, S30G20 and S13G75 biografts were executed by transformation of the osteoblast cells into bone cells. The differences were noticed on the daily basis of cell counts and the changes in the number of added cells were calculated (Figs. 11–13). Evaluation of cell viability of the biografts and the changes in the number of cells for different grafts was investigated. Figures 11a and b show the cell viability test results of the H30G20 and H13G75 porous biografts at different concentrations (0.1–0.3 μg/ml) by using osteoblast cell cultures. From the results it can be seen that, in both concentrations, the cell viability ratio was increased in both biografts. Figures 9a, b show the cell viability test results of the C30G20 and C13G75, and S-based S30G20 and S13G75 porous biografts were shown in Figs. 13a, b.

It was determined that the viability percent ratio at 0.1 μg/ml concentration changed linearly from the first day until the end of the third day for the S40G20 biograft. The live cell density was found well below the cell viability rate at a 0.3 μg/ml concentration, which is an indication of a toxic effect. However, the S10G75 biograft at both concentrations shows no toxicity and cell viability ratio is over 100 (Fig. 13b). Although all synthesized biografts contributed good mechanical properties – structure and cell viability results, considering both mechanical properties, results reveal that the synthesized C13G75 and S13G75 biografts provide the highest porosity (45–50%) and also generate better results considering the combination of porosity, mechanical properties (low elastic modulus and comparatively high strength), compared to the other synthesized biografts.

5. Conclusions

In this study, H-based, new porous bone grafts were synthesized by substituting cuttlefish backbone, sepiolite and gelatine and the following conclusions were summarized:

- Porous hydroxyapatite, cuttlefish bone and sepiolite-based biografts showed that as gelatin amount increased, the grain size and crystallinity of the grafts decreased.
- It was found that the porosity of hydroxyapatite, cuttlefish bone and sepiolite-based biografts increased as gelatin substitution increased.
- The highest porosity was obtained in the case of S13G75 (13 wt. % S, 12 wt. % H and 75 wt. % G) biograft (50.5%) and the lowest porosity was obtained in the case of H30G20 (30 wt. % H and 20 wt. % G, biograft (15.3%).
- The highest cell viability rate was found for the S13G75 biograft, which, having the highest porosity, suggests that the cell viability also increases in high-porous grafts.
- The synthesized biografts, except for the S40G20, which exhibits the lowest porosity, showed no toxicity effects.
- From the overall results, considering the mechanical properties and structure and *in vitro* cell viability tests together, the synthesized biografts C13G75 and S13G75 provided better correlation between porosity, mechanical property and cell viability rates.

References

[1] RODAN G.A., *Principles of Bone Biology*, 2nd ed., San Diego, Academic Press 2002.

[2] ZYSSET P.K., GUO X.E., HOFFLER C.E., MOORE K.E., GOLDSTEIN S.A., *Elastic modulus and hardness of cortical and trabecular bone lamellae measured by nanoindentation in the human femur*, J Biomech., 1999, 32, 10, 1005.

[3] KEAVENY T.M., MORGAN E.F., NIEBUR G.L., YEH O.C., *Biomechanics of Trabecular Bone*, Annu. Rev. Biomed. Eng., 2001, 3, 307.

[4] GREEN D., WALSH D., MANN S., OREFFO R.O.C., *The Potential of Biomimesis in Bone Tissue Engineering: Lessons from The Design and Synthesis of Invertebrate Skeletons*, Bone, 2002, 50, 253.

[5] LOWENSTAM H.A., WEINER S., *On Biomineralization*, Oxford Univ. Press, 1989.

[6] ROCHA J.H.G., LEMOS A.F., AGATHOPOULOS S., VALERIO P., KANNAN S., OKTAR F.N., FERREIRA J.M.F., *Scaffolds for Bone Restoration from Cuttlefish*, Bone, 2005, 37, 850.

[7] BALAZSI C., WEBER F., KÖVER Z., HORVATH E., NEMETH C., *Preparation of Calcium – Phosphate Bioceramics From Natural Resources*, J. Eur. Ceram. Soc., 2007, 27, 1601.

[8] ROCHA J.H.G., LEMOS A.F., AGATHOPOULOS S., KANNAN S., VALERIO P., FERREIRA J.M.F., *Hydrothermal Growth of Hydroxyapatite Scaffolds from Aragonitic Cuttlefish Bones*, Wiley Interscience, 2005.

[9] KANNAN S., ROCHA J.H.G., AGATHOPOULOS S., FERREIRA J.M.F., *Fluorine-Substituted Hydroxyapatite Scaffolds Hydrothermally Grown from Aragonitic Cuttlefish Bones*, Acta Biomaterialia, 2007, 3, 243.

[10] AKSAKAL B., DEMIREL M., *Synthesis and fabrication of novel cuttlefish (sepia officinalis) backbone biografts for biomedical applications*, Ceramics Int., 2015, 41(3), 4531.

[11] DEMIREL M., AKSAKAL B., *Synthesis of novel meerschaum (sepiolite) derived bioceramics versus hydroxyapatite based bone grafts*, Ceramics Int., 2015, 41, 9251.

[12] HENCH L.L., *Sol-Gel Materials for Bioceramic Applications*, Curr. Opin. Solid State Mater. Sci., 1997, 2, 604.

[13] JENKINS M., BOCA RATORN F.L., *Biomedical Polymers*, CRC Press, 2007.

[14] KARAGEORGIOU V., KAPLAN D., *Review: Porosity of 3D Biomaterial Scaffolds and Osteogenesis*, Biomaterials, 2005, 26, 5474.

[15] LIU X., MA P.X., *Phase Seperation, Pore Structure, and Properties of Nanofibrous Gelatin Scaffolds*, Biomaterials, 2009, 30, 4094.

[16] LIU X., SMITH L.A., HU J., MA P.X., *Biomimetric Nanofibrous Gelatin/Apatite Composite Scaffolds For Bone Tissue Engineering*, Biomaterials, 2009, 30, 2252.

[17] ZHANG Y.F., CHENG X.R., CHEN Y., SHI B., CHEN X.H., XU D.X., KE J., *Three-Dimensional Nanohydroxiapatite/Chitosan Scaffolds As Potential Tissue Engineered Periodontal Tissue*, J. Biomater. Appl., 2007, 21, 333.

[18] ZHAO F., GRAYSON W.L., MA T., BUNNELL B., LU W.W., *Effects of Hydroxiapatite in 3D Chitosan-Gelatin Polymer Network on Human Mesenchymal Stem Cell Construct Development*, Biomaterials, 2006, 27, 1859.

[19] MANJUBALA I., SCHELER S., BOSSERT J., JANDT K.D., *Mineralisation of Chitosan Scaffolds With Nano-Apatite Formation By Double Diffusion Technique*, Acta Biomater., 2006, 2, 75.

[20] TAKAHASHI Y., YAMAMOTO M., TABATA Y., *Osteogenic Differentation of Mesenchymal Stem Cell in Biodegradable Sponges Composed of Gelatin and β-Tricalcium Phosphate*, Biomaterials, 2005, 26, 3587.

[21] XU H.H., SIMON C.G., *Fast Setting CalciumPhosphate-Chitosan Scaffold: Mechanical Properties and Biocompatibility*, Biomaterials, 2005, 26, 1337.

[22] OLAH L., BORBAS L., *Properties of calcium carbonate – containing composite scaffolds*, Acta Bioeng Biomech., 2008, 10(1), 61–66.

[23] TRYBUŚ B., ZIELIŃSKI A., BEUTNER R., SERAMAK T., SCHARNWEBER D., *Deposition of phosphate coatings on titanium within scaffold structure*, Acta Bioeng. Biomech., 2017, 19(2), 65–72.

[24] LIU X. et al., *Surface nano-functionalization of biomaterials*, Materials Science and Engineering, 2010, R 70, 275.

[25] NAKONIECZNY D., PASZENDA Z., DREWNIAK S., RADKO T., LIS M., *ZrO_2-CeO_2 ceramic powders obtained from a sol-gel processusing acetylacetone as a chelating agent for potential application in prosthetic dentistry*, Acta of Bioeng. and Biomech., 2016, 18(3), 53–60.

[26] NAKONIECZNY D.S., PASZENDA Z.K., BASIAGA M., RADKO T., DREWNIAK S., PODWÓRNY J., BOGACZ W., *Phase composition and morphology characteristics of ceria-stabilized zirconia powders obtained via sol-gel method with various pH conditions*, Acta of Bioeng. and Biomech., 2017, 19(2), 21–30.

[27] JANUS et al., *Plasma assisted chemical vapour deposition – technological design of functional coatings*, Archives of Metallurgy and Materials, 2915, 60, 909.

[28] AKSAKAL B., SAY Y., BUYUKPINAR Ç., BAKIRDERE S., *Biodegradation of hydroxyapatite coated Rex-734 alloy with silver and selenium/chitosan substitutions: In vitro analysis*, Ceramics International, 2017, 43, 12609–615.

[29] WORD A.G., COURTS A., *The Science and Technology of Gelatin*, Academic Press. London 1977.

[30] NARASARAJU T.S.B., PHEBE D.E., *Some Physico-Chemical Aspects of Hydroxyapatite*, J. Mater. Sci., 1996, 31, 1.

[31] LEE S.H., SHIN H., *Matrices and Scaffolds for Delivery of Bioactive Molecules in Bone and Cartilage Tissue Engineering*, Adv. Drug. Delivery Rev., 2007, 59, 339.

[32] EVIS Z., WEBSTER T.J., *Nanosize hydroxyapatite: doping with various ions*, Adv. Appl. Cer: Struct. Funct. Biocer., 2011, 110, 311.